Density Functional Theory and X-ray Investigations of P- and M-Hexamethylene Triperoxide Diamine and Its Dialdehyde Derivative

Andrzej Wierzbicki,*,† E. Alan Salter, Eugene A. Cioffi,† and Edwin D. Stevens‡

Department of Chemistry, University of South Alabama, Mobile, Alabama 36688, and Department of Chemistry, University of New Orleans, New Orleans, Louisiana 70148

Received: June 21, 2001

Recently, we carried out a density functional theory B3LYP/6-31+G(d) study of hexamethylene triperoxide diamine (HMTD) in order to elucidate the unusual, nearly planar, sp^2 hybridization of the two bridgehead nitrogen atoms, each bonded to the three CH_2 groups. We postulated that extended bonding orbitals between peroxide oxygens results in charge delocalization which decreases lone-pair repulsion and compensates the energy loss due to the sp^3 to sp^2 hybridization change on the nitrogen atoms. We have reexamined the crystal structure of HMTD by performing low-temperature, single-crystal X-ray studies, and we have determined that the unit cell contains a 50−50 racemic mixture of enantiomeric forms of HMTD, showing disorder about the mirror plane. At the low temperature, all hydrogen atoms were located and resolved, which was not previously possible. We have also crystallized and performed low-temperature X-ray analysis of a never previously reported dialdehyde form of HMTD, tetramethylene diperoxide diamine dialdehyde (TMDDD), which reveals enantiomers present in the unit cell without disorder. B3LYP density functional theory studies of HMTD and TMDDD are presented, as well as a transition state investigation of possible thermal interconversion of the HMTD enantiomers.

Introduction

The explosive properties of 1,6-diaza-3,4,8,9,12,13-hexaoxabicyclo[4.4.4]tetradecane, hexamethylene triperoxide diamine (HMTD),

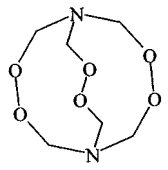

a powerful initiator belonging to the family of triperoxide energetic materials, have been known since the molecule was synthesized by Legler[1] in 1885. To our knowledge, HMTD's correct structural form was for the first time deduced/proposed by Urbanski.[2] The crystallographic structure reported by Schaefer et al.[3] revealed a planar 3-fold coordination about the two bridgehead nitrogen atoms. In our previous paper,[4] we reported that the Hartree−Fock (HF) and density functional theory (DFT) models also produce this unusual geometry in gas-phase calculations. Furthermore, we showed that HMTD has extended orbitals, which allow charge delocalization and thus decreased repulsion between lone-pair electrons on the oxygen atoms. Also, the lone-pair repulsion of the nitrogen atoms is lessened by a bonding orbital which extends over a 3.4 Å distance. These extended orbitals are made possible by the overlaps afforded by the cage structure, and we concluded that the energy loss due to the sp^3 to sp^2 hybridization change on the nitrogen atoms is compensated in this way. The crystal structure of HMTD showed another interesting feature: the structure was disordered about the mirror plane imposed by the choice of space group *R*3*m*. When other authors presented the asymmetric unit of HMTD derived from their X-ray data[3] (see their Figures 1 and 2), they showed the three peroxide bonds in a helical pattern, akin to the right-handed "barber pole" design; no mention was made of a possible left-handed isomer. While setting up earlier calculations for HMTD,[4] we entirely ignored the left-handed form, mainly because the information pertaining to the disorder was buried in the body of the text. When we realized from our computational tests that HMTD must indeed be enantiomeric, a fact which has been never mentioned in the literature, we became very interested in analyzing the transition path between the right- and left-handed forms.

We have broadened our original DFT study to explore stable chiral forms of HMTD, and we have carried out transition state searches to elucidate possible thermal interconversion between them. At the same time, we have undertaken several attempts to recrystallize HMTD in order to unequivocally resolve the two most stable chiral forms without superposition. Although we were unable to "separate" the chiral forms within the unit cell, our X-ray analysis indicates that the crystal is indeed a 50−50 racemic mixture, and our efforts resulted in a much better resolved X-ray structure, obtained at 150 K, which will be discussed in this paper. The original X-ray structure[3] showed a large discrepancy between the top (N2 side) and bottom (N1 side) values for the structural parameters of HMTD (Table 1 in Schaefer et al.[3]). This discrepancy was so significant that in our original calculations[4] we did not feel justified in using any symmetry constraints. Our new X-ray analysis revealed a structure that is much closer to D_3 symmetry (Table 1) and this symmetry was used for HMTD calculations discussed in this paper. Additionally in our X-ray structure, for the first time, all of the (disordered) hydrogen atoms were located and resolved, providing further confirmation of the disordered arrangement of the molecules in the solid state.

† University of South Alabama.
‡ University of New Orleans.

10.1021/jp0123841 CCC: $20.00
Published on Web 08/30/2001

A recrystallization attempt in which the HMTD solution was fortuitously exposed to air yielded crystals of a dialdehyde derivative of HMTD, 1,2,6,7,4,9-tetraoxadiazaperhydroecine-4,9-dicarbaldehyde, tetramethylene diperoxide diamine dialdehyde (TMDDD).

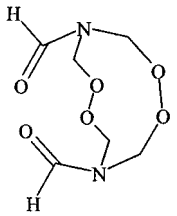

X-ray analysis of a single crystal reveals left- and right-handed forms of TMDDD present in the unit cell, fully resolved, without disorder. The TMDDD molecule exhibits a nearly planar 3-fold coordination about the two bridgehead (amide) nitrogen atoms. Our DFT calculations show that lone-pair delocalization in TMDDD is similar to that of HMTD.

Computational Details

Density functional calculations using *Gaussian98*[5] were carried out on Cray SV1 and SGI Octane 300 computers. In all-electron calculations, we employed the Becke hybrid three-parameter DFT method[6] using the Lee, Yang, and Parr correlation functional[7] (B3LYP) and the 6-31+G(d) polarized split-valence basis set[8−13] which includes diffuse functions, as recommended for the description of lone-pair electrons. The default grid option was chosen for numerical integration of matrix elements, except when explicitly mentioned otherwise. Calculations for HMTD involved a total of 110 electrons with 290 contracted Gaussian basis functions consisting of 496 primitive Gaussians. Preliminary HF and subsequent DFT optimizations of TMDDD involved a total of 108 electrons with 286 contracted Gaussian basis functions consisting of 488 primitive Gaussians. C_1 symmetry was used throughout full optimizations and subsequent frequency calculations. D_3 symmetry was imposed where stated for HMTD, in a follow-up optimization. Analytic harmonic vibrational frequencies were computed for all structures to confirm that local minima (or transition states) on the potential-energy surface had been found.

Experimental geometries were obtained from X-ray-derived coordinates, contained in the crystallographic information files using the materials science modeling software *Cerius*[2] (ver. 4.2MS).[14] Molecular graphics were generated using *Spartan*[15] (ver. 5.1.1) interface for *Gaussian98*.

Experimental Details

Unlabeled hexamethylenetetramine (hexamine; Aldrich Chemical Co., # 39,816-0) was purified via bulb-to-bulb sublimation, 165−175° (3.0 mm): mp 263−264 °C (lit. mp = 263 °C[16]); ^{1}H NMR ($CDCl_3$) δ 4.73; ^{13}C NMR δ 74.99.

Synthesis of Hexamethylene Triperoxide Diamine (HMTD). *Caution: HMTD is a powerful explosive.* A 125 mL three-neck flask equipped with a paddle-type microstirrer was charged with 7.00 g (50 mmol) of hexamethylenetetramine and 23 mL of 50% H_2O_2 and chilled to ~0 °C (ice/NaCl). While being stirred, 11.5 g (54.7 mmol) citric acid monohydrate was added in 10 small portions over the course of 2 h. The clear solution was stirred at ~0 °C for an additional 8 h; the ice-bath was removed, and the solution was allowed to warm slowly to room temperature. The resultant opaque mixture was stirred for an additional 2 h, the micro-stirrer was removed, and the flask containing the product was re-chilled in ice for 30 min. The white crystalline material was gravity filtered and then rinsed with 3 × 50 mL ice water, followed by 2 × 20 mL ice-cold CH_3OH rinses. The crystalline material and filter paper was dried in a vacuum desiccator ($CaSO_4$) overnight to afford 5.75 g (27.6 mmol; 55%) product: mp = 152−153 °C (exp.) (lit. mp = 144−145 °C;[17] 154 °C[18]); ^{1}H NMR ($CDCl_3$): δ 4.80; ^{13}C NMR δ 90.44.

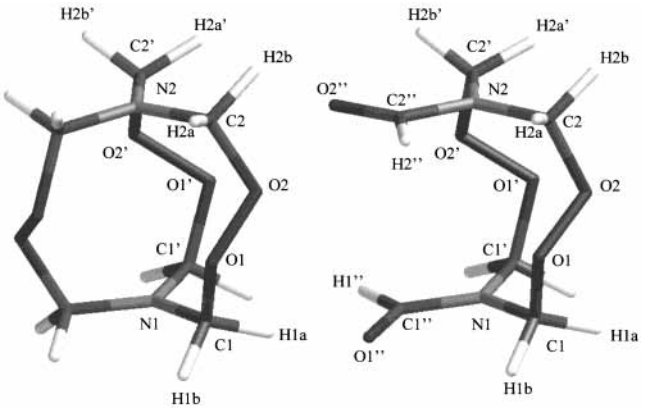

Figure 1. HMTD and TMDDD geometry and atom labeling. P enantiomers are shown; that is, all peroxide bonds are dextral relative to the N_1-N_2 axis.

Synthesis of Tetramethylene Diperoxide Diamine Dialdehyde (TMDDD). *Caution: TMDDD is an explosive material.* A 250 mL Erlenmeyer flask equipped with a stirring bar was charged with ~100 mL *n*-butyl acetate and brought to a gentle boil. To this hot stirred solvent was added 0.5011 g (2.4 mmol) of HMTD in portions until the HMTD had completely dissolved. This mixture was purged with a gentle stream of O_2 via a capillary for 5 min, removed from heating, and allowed to cool to room temperature. The crystalline white product was filtered, dried under vacuum, and re-crystallized (*n*-BuOAc): mp = 155 °C (exp.); ^{1}H NMR ($DMSO_{d-6}$) δ 8.08 (s, 1H), 5.12 (dd, 2H), 5.08 (dd, 2H); ^{13}C NMR δ 165.18 (C=O), 81.68 (CH_2), 78.48 (CH_2). Calculated: $C_6H_{10}O_6N_2$: 34.96% C, 4.89% H, 13.59% N. Found: 35.01% C, 4.94% H, 13.68% N.

Melting points were taken on a Hoover-Thomas capillary apparatus and are uncorrected. Proton (^{1}H) and carbon-13 (^{13}C) NMR spectra were run on a JEOL GFX-300 spectrometer using either $CDCl_3$ or $(CD_3)_2SO$ with TMS as an internal reference. Elemental microanalysis was performed by Atlantic Microlab, Inc., Norcross, GA 30071.

X-ray Data Collection and Refinement. Crystals of HMTD and TMDDD were attached to glass fibers using silicone vacuum grease, mounted on a Brüker SMART 1K CCD automated diffractometer, and cooled to 150(2) K in a stream of cold N_2 gas. Data were collected using two ω-scans on each crystal over a 180° range at φ = 0° and 90° with 0.30° scan width and 60 s count time per frame and a crystal-to-detector distance of 3.50 cm. The structures were solved by direct methods and refined by full-matrix least-squares techniques. The positions of all hydrogen atoms were located and included in the refinement with isotropic thermal parameters.

Results and Discussion

The structural parameters of HMTD and TMDDD as determined by experiment and the *Gaussian98* implementations of the B3LYP and HF models are summarized in Table 1. Corresponding atom labels are shown in Figure 1. Experimental bond lengths, bond angles, and dihedrals were obtained from

the coordinates determined by X-ray analysis contained in the crystallographic information file. Tables 2 and 3 contain the crystal data and structure refinement information for HMTD and TMDDD, respectively. As reported previously,[3] the structure of HMTD in space group *R*3*m* is disordered, showing a superposition of molecules with both left and right twists. This is also evident in the hydrogen positions, which could be located even in the presence of the disorder. Equal population of the two forms is imposed by a crystallographic mirror plane. Refinement of the structure in space group *R*3, which does not impose a mirror plane on the model, was successful but yielded a refined occupancy factor of 0.500(1) for each of the two forms, indicating that the crystal is truly a racemic mixture of the two forms of the molecule. Since the agreement factors are not significantly improved in space group *R*3 after considering the increase in parameters, the final structure is reported in *R*3*m*. An ORTEP drawing of the two HMTD forms present in the unit cell is shown in Figure 2. For the sake of brevity, we will call them M- and P-HMTD according to the helical direction of the three peroxide bonds. The adjacent C−O bonds are in the opposite direction of the peroxide bonds; the full description of the C−O−O−C bond sequence is M, P, M for what we call P-HMTD. The unit cell contains six superimposed pairs of P and M forms.

Successful refinement of the TMDDD structure was achieved in space group $Pna2_1$ without disorder. Two enantiomers, one of which constitutes the asymmetric unit and the other generated by a crystallographic glide plane, we call P- and M-TMDDD. They are found to be fully ordered in the cell; the unit cell contains two P and two M units, and the crystal is a 50−50 racemic mixture. Figure 3 shows an ORTEP drawing of the P-TMDDD enantiomer. Both HMTD and TMDDD experimental structures show small asymmetry between lower (atomic indices 1) and upper (atomic indices 2) parts. The broken symmetry of HMTD is less pronounced in our new X-ray structure, as compared to earlier data,[3] but it is nevertheless present. TMDDD is almost planar at the bridgehead nitrogens; only a very slight *in*, *in* puckering is observed. To illustrate, the C1−N1−C1′ and C2−N2−C2′ angles are 119.8° and 121.4°, for example. Both angles are 120.0° in HMTD.

With regard to the disorder of the HMTD structure, we believe that during crystal packing, the barrel-shaped M and P forms of HMTD can be randomly placed, since the intermolecular interactions only very weakly distinguish these closed

TABLE 1: Comparison of Experimental and Calculated Structural Parameters of HMTD and TMDDD

bond/angle[a]	HMTD exptl, room temp[b]	HMTD exptl, 150 K	HMTD B3LYP/ 6-31+G(d)[c]	HMTD B3LYP/ 6-31+G(d)[d]	TMDDD exptl, 150K	TMDDD HF/ 6-31+G(d)[e]	TMDDD B3LYP/ 6-31+G(d)[e]
N1−Cl	1.426(8)	1.4272(11)	1.435	1.435	1.452(3)	1.438	1.449
N2−C2′	1.417	1.4242(7)	1.435	1.435	1.445(3)	1.438	1.449
O1−O2	1.456(8)	1.4696(11)	1.459	1.459	1.469(2)	1.392	1.464
C1−O1	1.410	1.4315(14)	1.427	1.427	1.418(3)	1.398	1.418
C2′-O2′	1.432	1.4438(10)	1.427	1.427	1.414(2)	1.398	1.418
N1−C1″					1.351(3)	1.369	1.385
N2−C2″					1.359(3)	1.369	1.385
C1″−O1″					1.209(3)	1.193	1.216
C2″−O2″					1.210(3)	1.193	1.216
C1″−H1″					0.91(3)	1.087	1.103
C2″−H2″					1.00(3)	1.087	1.103
C1−N1−C1′	120.0(5)	119.999(1)	119.94	119.93	119.80(19)	121.34	121.41
C2−N2−C2′	120.0(5)	119.960(3)	119.92	119.93	121.35(17)	121.34	121.41
N1−C1−O1	116.6(5)	116.48(9)	117.85	117.90	113.44(17)	114.43	115.13
C1−O1−O2	107.3(5)	106.49(7)	107.29	107.29	106.27(14)	107.97	107.00
O1−O2−C2	105.2(5)	104.59(5)	107.31	107.29	106.20(14)	107.97	106.65
O2−C2−N2	115.7(5)	115.90(6)	117.89	117.90	113.93(16)	115.16	115.84
N1−N2	3.294	3.297(1)	3.411	3.415	3.278(2)	3.421	3.473
C1−O1−O2−C2	129.3(5)	128.98(10)	129.35	±129.47	132.04(18)	137.36	136.09
C1−H1a	0.950	0.987(15)	1.096	1.097	1.00(3)	1.080	1.094
C1−H1b	0.950	0.929(17)	1.097	1.097	0.94(2)	1.077	1.093
C2′−H2a′	0.951	1.05(2)	1.096	1.097	1.01(3)	1.081	1.094
C2′−H2b′	0.950	0.842(19)	1.097	1.097	1.03(3)	1.077	1.093
N1−C1″−O1″					124.0(2)	124.09	124.18
N2−C2″−O2″					124.1(2)	124.09	124.18
N1−C1″−H1″					115.9(14)	113.55	112.95
N2−C2″−H2″					112.3(16)	113.55	112.95
C1−N1−C1″					119.05(16)	118.20	118.19
C2′−N2−C2″					118.01(18)	118.20	118.19
H1a−C1−H1b	109.49	106.2(14)	109.84	109.84	111(2)	110.83	111.17
H2a′−C2′−H2b′	109.40	112.9(15)	109.85	109.84	111(2)	110.83	111.17
N1−C1−H1a	107.65	109.3(10)	108.81	108.80	111.3(14)	109.22	109.25
N1−C1−H1b	107.66	108.3(10)	110.27	110.23	108.2(14)	109.33	108.99
N2−C2′−H2a′	107.86	106.7(13)	108.81	108.80	109.4(16)	109.22	109.25
N2−C2′−H2b′	107.82	112.9(15)	110.24	110.23	109.6(13)	109.33	108.99
O1−O1′	3.585	3.614(1)	3.612	3.606	3.607(2)	3.481	3.552
O1−O2′	4.127	4.164(1)	4.140	4.137	4.112(2)	3.912	4.019
O2−O2′	3.608	3.644(1)	3.606	3.606	3.622(2)	3.481	3.552
N1−C1−O1−O2	−72.65	−73.48(12)	−71.03	∓71.27	−77.2(2)	−75.27	−75.64
C1″−C2″					3.318(3)	3.572	3.670
C1−C2	3.339	3.356(1)	3.376	3.377	3.368(3)	3.345	3.399

[a] Bond lengths and other distances are in angstroms, and bond angles and dihedral angles are in degrees. [b] Experimental data from earlier work.[3] Values for which no esd is given are derived from the fractional coordinate data file. [c] Previously reported.[4] [d] Both P and M enantiomers are represented. D_3 symmetry is imposed. Grid = 99590 option was employed to recover P/M degeneracy. [e] C_2 symmetry is present but not imposed.

TABLE 2: Crystal Data and Structure Refinement for HMTD

identification code	hmtd	
empirical formula	$C_6H_{12}N_2O_6$	
formula weight	208.18	
temperature	150(2) K	
wavelength	0.710 73 Å	
crystal system	rhombohedral	
space group	*R*3*m*	
unit cell dimensions	$a = 10.3982(4)$ Å	$\alpha = 90°$
	$b = 10.3982(4)$ Å	$\beta = 90°$
	$c = 6.9332(4)$ Å	$\gamma = 120°$
volume	649.20(5) Å^3	
Z	3	
density (calculated)	1.597 Mg/m^3	
absorption coefficient	0.144 mm^{-1}	
F(000)	330	
crystal size	0.40 × 0.30 × 0.25 mm^3	
θ range for data collection	3.71−34.85°	
index ranges	$-16 \le h \le 16$, $-16 \le k \le 16$, $-10 \le l \le 10$	
reflections collected	4578	
independent reflections	695 [R(int) = 0.0212]	
completeness to $\theta = 34.85°$	98.3%	
absorption correction	empirical	
max. and min. transmission	1.0000 and 0.7498	
refinement method	full-matrix least-squares on F^2	
data/restraints/parameters	695/10/56	
goodness-of-fit on F^2	1.038	
final R indices [$I > 2\sigma(I)$]	$R_1 = 0.0217$, w$R_2 = 0.0521$	
R indices (all data)	$R_1 = 0.0242$, w$R_2 = 0.0531$	
absolute structure parameter	0.1	
largest diff. peak and hole	0.148 and −0.100 e Å^{-3}	

TABLE 3: Crystal Data and Structure Refinement for TMDDD

identification code	usa2m	
empirical formula	$C_6H_{10}N_2O_6$	
formula weight	206.16	
temperature	150(2) K	
wavelength	0.71073 Å	
crystal system	orthorhombic	
space group	$Pna2_1$	
unit cell dimensions	$a = 8.0807(6)$ Å	$\alpha = 90°$
	$b = 10.2592(7)$ Å	$\beta = 90°$
	$c = 10.4064(7)$ Å	$\gamma = 90°$
volume	862.71(10) Å^3	
Z	4	
density (calculated)	1.587 Mg/m^3	
absorption coefficient	0.143 mm^{-1}	
F(000)	432	
crystal size	0.40 × 0.40 × 0.50 mm^3	
θ range for data collection	2.79−23.75°	
index ranges	$-9 \le h \le 7$, $-11 \le k \le 7$, $-10 \le l \le 11$	
reflections collected	3311	
independent reflections	1173 [R(int) = 0.0450]	
completeness to $\theta = 23.75°$	100.0%	
absorption correction	none	
refinement method	full-matrix least-squares on F^2	
data/restraints/parameters	1173/1/167	
goodness-of-fit on F^2	1.048	
final R indices [$I > 2\sigma(I)$]	$R_1 = 0.0275$, w$R_2 = 0.0726$	
R indices (all data)	$R_1 = 0.0282$, w$R_2 = 0.0730$	
absolute structure parameter	−0.8(11)	
largest diff. peak and hole	0.214 and −0.168 e Å^{-3}	

cage shapes. On the other hand, the more distinguishable chiral interactions of M- and P-TMDDD require orderly packing to achieve minimum crystal energy. Apparently, crystal packing causes some pinching of the aldehyde moieties of TMDDD: the C1″−C2″ distance is about 0.05 Å less than the C1−C2 distance.

Since each of the forms of HMTD have C_1 symmetry due to slight differences between the geometry in the upper versus the lower parts of the molecule, we first conducted the standard grid DFT geometry optimization without symmetry constraints. The previously reported P-HMTD geometry[4] is summarized in the third column of Table 1. The new X-ray-determined HMTD geometry reported in this paper is much closer to D_3 symmetry, so we imposed symmetry, employed a finer grid, and reoptimized. The dependence of DFT methods on a computational grid leads to loss of rotational invariance, and a finer grid was necessary to recover the degeneracy of the right- and left-handed

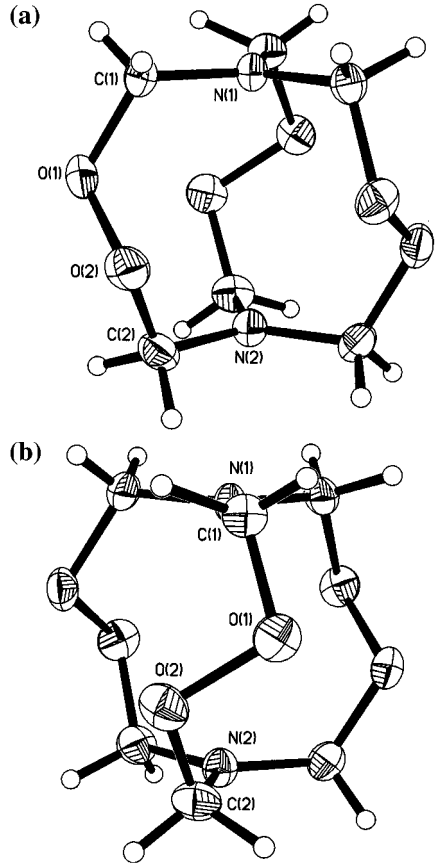

Figure 2. ORTEP drawing of (a) M-HMTD and (b) P-HMTD. Thermal ellipsoids enclose 50% of the atomic probability. Atom labeling corresponds to crystallographic data provided in the Supporting Information.

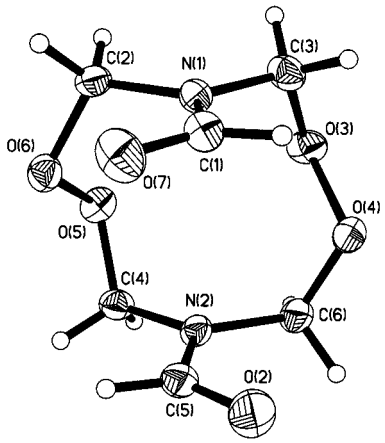

Figure 3. ORTEP drawing of P-TMDDD. The peroxide bonds are dextral relative to the N−N axis. The space group $Pna2_1$ includes glide plane operations which change P- to M-TMDDD within the unit cell. Thermal ellipsoids enclose 50% of the atomic probability. Atom labeling corresponds to crystallographic data provided in the Supporting Information.

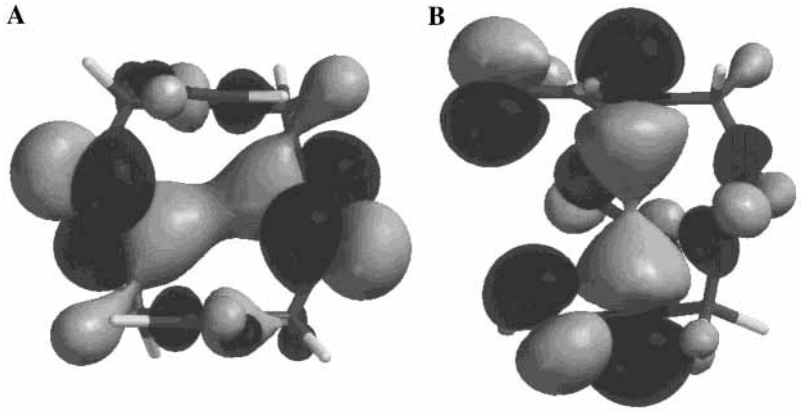

Figure 4. (A) HOMO-3 and (B) HOMO-4 of TMDDD.

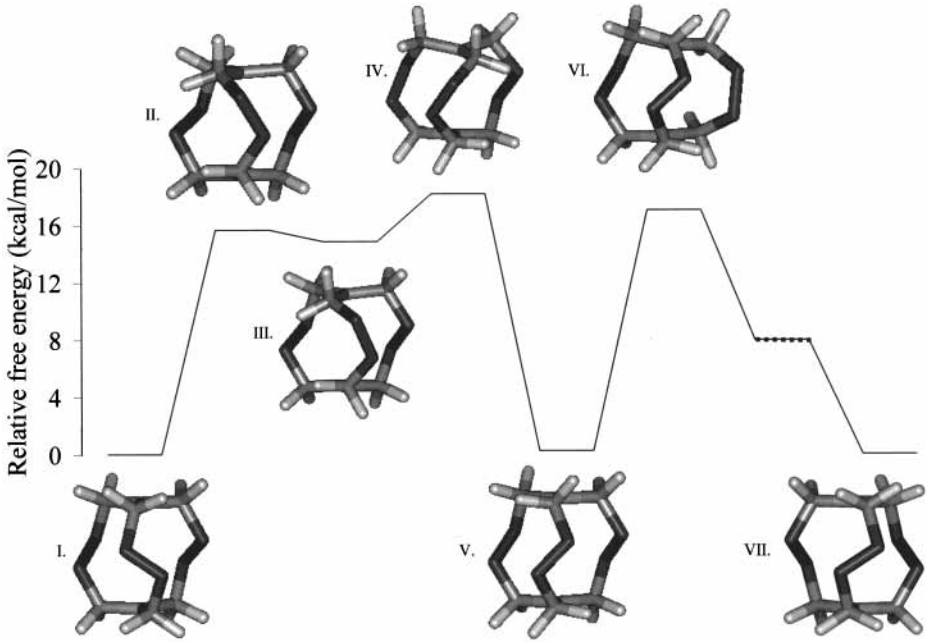

Figure 5. Potential energy surface showing interconversion of M- and P-HMTD. Free energies are computed relative to the energy of M- and P-HMTD at 298 K using the B3LYP/6-31+G(d) model. I. M-HMTD. All peroxide bonds are sinister. **II**. Transition state at 16 kcal/mol. Structure is the result of disrotatory motion of a pair of C−N bonds. **III**. Intermediate structure at 15 kcal/mol. **IV**. Transition state at 18 kcal/mol. Structure is the result of disrotatory motion in the reverse sense of the first step. **V**. M-iso-HMTD. This structure is only slightly higher in energy (0.3 kcal/mol) than M- and P-HMTD. One peroxide bond (middle) is dextral; the other two are sinister. This structure was achieved from IV ostensibly by solo rotation of the upper C−N bond. **VI**. Transition state at 17 kcal/mol. Structure is the result of disrotatory motion of the pair of C−N bonds at right, but with emphasis on rotation of the lower bond. This transition state leads directly to P-iso-HMTD (not shown), the enantiomer of V. **VII**. P-HMTD. The remaining surface (indicated by dots) includes the mirror images of V, IV, III, and II on the way to VII (P-HMTD), in which all peroxide bonds are dextral.

optimized structures. Optimized P- and M-HMTD structures are summarized by the data in column four. We conclude that the isolated enantiomers possess D_3 symmetry, but that in the solid phase, either crystal packing forces or experimental uncertainties result in the observed C_1 symmetry. We conclude the same in regard to the observed C_1 symmetry of TMDDD; our DFT calculations indicate that the TMDDD enantiomers possess C_2 symmetry in isolation.

An excellent agreement in the overall calculated structures for HMTD and TMDDD has been achieved with the DFT model, when compared to the new experimental data, as seen in Table 1. Most calculated bond lengths are slightly longer, which is expected for the B3LYP/6-31+G(d) model.[19] Bond angles and dihedral angles are remarkably well reproduced. Comparison of DFT and HF results for TMDDD clearly indicates that the Hartree−Fock level is sufficient for the general structural determination of this lone-pair-rich molecule, with the exception of the oxygen−oxygen interaction distances. In particular, the O1−O2 bond length is estimated poorly by the Hartree−Fock model and quite well by the B3LYP model. We concluded before for HMTD that this shortcoming of the HF model reflects its lack of correlation effects.[4] The computed value of the C1″−C2″ distance is longer than the C1−C2 distance by 0.27 Å in TMDDD, with the aldehyde groups slightly bent away from one another, as would be expected in the gas phase. Previously, we showed that the unusual, planar geometry of the nitrogen atoms is successfully reproduced in the B3LYP/6-31+G(d) model for HMTD, and we reported that extended orbitals tend to delocalize the lone-pairs of the peroxide oxygens. Also, the lone-pair repulsion of the bridgehead nitrogens is lessened by an orbital which is largely the plus combination of the p_z orbitals and achieves delocalization within the body of the cage.[4] The HOMO-3 and HOMO-4 Kohn−Sham DFT orbitals of TMDDD (Figure 4) correspond to the HOMO-1/HOMO-2 pair and HOMO-3 of HMTD, respectively (Figure 2 in earlier work[4]). The delocalization achieved by the

HOMO-4 of TMDDD (extending over 3.3 Å) is less than that of its counterpart. Other orbitals show significant delocalization of the lone pairs in both molecules. In TMDDD, the nitrogen lone-pairs are involved in the carbonyl π bond; substitution of the carbonyl causes loss of planarity in computational models. We conclude that the cagelike structure of TMDDD permits the formation of extended delocalized bonding orbitals similar to those seen in HMTD.

Given the softness of the peroxide bonds, an investigation of possible thermal interconversion between the right- and left-handed forms of HMTD at or below room temperature seemed appropriate. Attempts to find a single transition state in which the orientations of all three peroxide bonds reverse simultaneously were not successful. However, a multistep pathway illustrated in Figure 5 was revealed.

In M-HMTD (I), all three peroxide bonds have a sinister orientation about the N−N axis. The reversal of one peroxide bond to the dextral orientation occurs in two steps: first, to intermediate **III** via transition state **II**, and second, to what we call M-iso-HMTD (**V**) via transition state **IV**. **V** is a stable structure only about 0.3 kcal/mol higher in energy than the P- and M-HMTD enantiomers (**I** and **VII**). One of the two remaining sinister peroxide bonds of **V** is reversed to yield the enantiomer of **V**, P-iso-HMTD (not shown), via transition state **VI**. Finally, the orientation of the remaining sinister peroxide bond is reversed to obtain P-HMTD (**VII**) in two steps, mirroring the **I** to **III** and **III** to **V** steps. The barriers of about 16−17 kcal/mol suggest that thermal interconversion may occur at room temperature.

Conclusions

We have extended our computational density functional theory investigation of the chiral HMTD molecule, and we have explored the structural and electronic properties of a chiral dialdehyde derivative of HMTD, TMDDD. We report low-temperature X-ray data in which all atoms were crystallographically resolved for both compounds. Compared with the previously reported structure of HMTD,[3] the current low-temperature study includes significantly more observations (695 vs 155). The resulting estimated standard deviations in the structural parameters are reduced by a factor of 6−11, and all of the (disordered) hydrogen atoms were located and refined, providing further conformation of the disordered arrangement of the molecules in the solid state. The chiral forms of TMDDD are fully resolved in the unit cell, while the unit cell of HMTD shows a random superposition of enantiomers. The never previously reported partial cage structure of TMDDD is similar to that of HMTD, and it affords similar lone-pair delocalization though extended orbitals (Figure 4). Also, DFT calculations were used to investigate the nature of the transition states that connect the chiral forms of HMTD. We find the barriers to interconversion using the B3LYP/6-31+G(d) model low enough (16−17 kcal/mol) to allow racemization at room temperature, and we conclude that the synthesis of a single enantiomer is unlikely.

Acknowledgment. We thank the Alabama Supercomputer Authority and Nichols Corporations for providing computer time on Cray SV1.

Supporting Information Available: CIF files pertaining to the HMTD and TMDDD. This material is available free of charge via the Internet at http://pubs.acs.org.

References and Notes

(1) Legler, L. *Ber.* **1885**, *18*, 3343.
(2) Urbanski, T. Presented at the International Symposium on the Chemistry of Organic Peroxides, Berlin-Adlershof, September, 1967.
(3) Schaefer, W. P.; Fourkas, J.; Tiemann, T. B. J. *J. Am. Chem. Soc.* **1985**, *107*, 2461.
(4) Wierzbicki, A.; Cioffi, E. *J. Phys. Chem. A.* **1999**, *103*, 8890.
(5) Frisch, M. J.; Trucks, G. W.; Schlegel, H. B.; Scuseria, G. E.; Robb, M. A.; Cheeseman, J. R.; Zakrzewski, V. G.; Montgomery, J. A., Jr.; Stratmann, R. E.; Burant, J. C.; Dapprich, S.; Millam, J. M.; Daniels, A. D.; Kudin, K. N.; Strain, M. C.; Farkas, O.; Tomasi, J.; Barone, V.; Cossi, M.; Cammi, R.; Mennucci, B., Pomelli, C., Adamo, C.; Clifford, S.; Ochterski, J.; Petersson, G. A.; Ayala, P. Y.; Cui, Q.; Morokuma, K.; Malick, D. K.; Rabuck, A. D.; Raghavachari, K.; Foresman, J. B.; Cioslowski, J.; Ortiz, J. V.; Stefanov, B. B.; Liu, G.; Liashenko, A.; Piskorz, P.; Komaromi, I.; Gomperts, R.; Martin, R. L.; Fox, D. J.; Keith, T.; Al-Laham, M. A.; Peng, C. Y.; Nanayakkara, A.; Gonzalez, C.; Challacombe, M.; Gill, P. M. W.; Johnson, B.; Chen, W.; Wong, M. W.; Andres, J. L.; Gonzalez, C.; Head-Gordon, M.; Replogle, E. S.; Pople, J. A. *Gaussian 98*, rev. A.6; Gaussian Inc.: Pittsburgh, PA, 1998.
(6) Becke, A. D. *J. Chem. Phys.* **1993**, *98*, 5648.
(7) Parr, T. G.; Yang, W. *Density-Functional Theory of Atoms and Molecules*; Oxford University Press: New York, 1989.
(8) Ditchfield, R.; Hehre, W. J.; Pople, J. A. *J. Chem. Phys.* **1971**, *54*, 724.
(9) Hehre, W. J.; Ditchfield, R.; Pople, J. A. *J. Chem. Phys.* **1972**, *56*, 2257.
(10) Hariharan, P. C.; Pople, J. A. *Mol. Phys.* **1974**, *27*, 209.
(11) Gordon, M. S. *Chem. Phys. Lett.* **1980**, *76*, 163.
(12) Hariharan, P. C.; Pople, J. A. *Theo. Chim. Acta* **1973**, *28*, 213.
(13) Clark, T.; Chandrasekhar, J.; Spitznagel, G. W.; Schleyer, P. v. R. *J. Comput. Chem.* **1983**, *4*, 294.
(14) *Cerius*^{2}, ver. 3.5; Molecular Simulations, Inc.: San Diego, CA, 1997.
(15) *Spartan*, ver. 4.1.1; Wavefunction, Inc.: Irvine, CA, 1996.
(16) Nielsen, A. T.; Moore, D. W.; Ogan, M. D.; Atkins, R. L. *J. Org. Chem.* **1979**, *44*, 1678.
(17) Sülzle, D.; Klaeboe, P. *Acta Chem. Scand.* **1988**, *42*, 165.
(18) Vennerstrom, J. L. *J. Med. Chem.* **1989**, *32*, 64.
(19) Foresman, J. B.; Frisch, A. *Exploring Chemistry with Electronic Structure Methods*, 2nd ed.; Gaussian, Inc.: Pittsburgh, PA 1996.